Theses and Dissertations　　　　　　　　　　1. Thesis and Dissertation Collection, all items

2019-06

WAVE RUNUP ON A STEEP ROCKY BEACH WITH A SMALL RIVER PLUME

Xiong, Ka

Monterey, CA; Naval Postgraduate School

NAVAL POSTGRADUATE SCHOOL

MONTEREY, CALIFORNIA

THESIS

WAVE RUNUP ON A STEEP ROCKY BEACH WITH A SMALL RIVER PLUME

by

Ka Xiong

June 2019

Thesis Advisor: Mara S. Orescanin
Second Reader: Derek Olson

Approved for public release. Distribution is unlimited.

THIS PAGE INTENTIONALLY LEFT BLANK

REPORT DOCUMENTATION PAGE		*Form Approved OMB No. 0704-0188*

1. AGENCY USE ONLY *(Leave blank)*	2. REPORT DATE June 2019	3. REPORT TYPE AND DATES COVERED Master's thesis
4. TITLE AND SUBTITLE WAVE RUNUP ON A STEEP ROCKY BEACH WITH A SMALL RIVER PLUME		5. FUNDING NUMBERS
6. AUTHOR(S) Ka Xiong		
7. PERFORMING ORGANIZATION NAME(S) AND ADDRESS(ES) Naval Postgraduate School Monterey, CA 93943-5000		8. PERFORMING ORGANIZATION REPORT NUMBER
9. SPONSORING / MONITORING AGENCY NAME(S) AND ADDRESS(ES) N/A		10. SPONSORING / MONITORING AGENCY REPORT NUMBER
11. SUPPLEMENTARY NOTES The views expressed in this thesis are those of the author and do not reflect the official policy or position of the Department of Defense or the U.S. Government.		
12a. DISTRIBUTION / AVAILABILITY STATEMENT Approved for public release. Distribution is unlimited.		12b. DISTRIBUTION CODE A

13. ABSTRACT (maximum 200 words)

To date, there are limited in situ data collected on the coast and at river deltas because the ocean–land convergence boundary is highly energetic and presents significant difficulties for experimentation. The focus of most river discharge research has been on large river deltas, and less attention has been paid toward small river plumes. Similarly, the surf zone on steep rocky beaches is also a less-studied topic because of logistical challenges. In the present study, we use remote sensing techniques to observe and collect wave runup at Carmel River State Beach, a steep beach with varying coastline features. The focus of this research was to investigate vertical-wave runup on a steep rocky beach with a small river plume. Elevation data collected showed Carmel River State Beach is very uniform in slope across the shore. Time-stack image analysis of wave runup at different sections of the beach showed that contrary to Battjes' relationship between wave height and beach slope, near the Carmel River plume the greatest slope does not yield the highest vertical runup. Runup is affected by the hydrodynamics of river plume and coastal roughness by lowering the vertical height. The highest runup was observed on the sandy portion of beach, trailed by rocky shores, then river discharge. The empirical coefficients developed by Ahrens over smooth and rocky structured slopes produced runup values comparable to only those portions of the beach that had similar beach features.

14. SUBJECT TERMS Carmel, river, plume, swash, runup			15. NUMBER OF PAGES 53
			16. PRICE CODE
17. SECURITY CLASSIFICATION OF REPORT Unclassified	18. SECURITY CLASSIFICATION OF THIS PAGE Unclassified	19. SECURITY CLASSIFICATION OF ABSTRACT Unclassified	20. LIMITATION OF ABSTRACT UU

THIS PAGE INTENTIONALLY LEFT BLANK

Approved for public release. Distribution is unlimited.

WAVE RUNUP ON A STEEP ROCKY BEACH WITH A SMALL RIVER PLUME

Ka Xiong
Lieutenant Commander, United States Navy
BS, U.S. Naval Academy, 2009

Submitted in partial fulfillment of the
requirements for the degree of

**MASTER OF SCIENCE IN METEOROLOGY AND PHYSICAL
OCEANOGRAPHY**

from the

**NAVAL POSTGRADUATE SCHOOL
June 2019**

Approved by: Mara S. Orescanin
Advisor

Derek Olson
Second Reader

Peter C. Chu
Chair, Department of Oceanography

iii

THIS PAGE INTENTIONALLY LEFT BLANK

ABSTRACT

To date, there are limited in situ data collected on the coast and at river deltas because the ocean–land convergence boundary is highly energetic and presents significant difficulties for experimentation. The focus of most river discharge research has been on large river deltas, and less attention has been paid toward small river plumes. Similarly, the surf zone on steep rocky beaches is also a less-studied topic because of logistical challenges. In the present study, we use remote sensing techniques to observe and collect wave runup at Carmel River State Beach, a steep beach with varying coastline features. The focus of this research was to investigate vertical-wave runup on a steep rocky beach with a small river plume. Elevation data collected showed Carmel River State Beach is very uniform in slope across the shore. Time-stack image analysis of wave runup at different sections of the beach showed that contrary to Battjes' relationship between wave height and beach slope, near the Carmel River plume the greatest slope does not yield the highest vertical runup. Runup is affected by the hydrodynamics of river plume and coastal roughness by lowering the vertical height. The highest runup was observed on the sandy portion of beach, trailed by rocky shores, then river discharge. The empirical coefficients developed by Ahrens over smooth and rocky structured slopes produced runup values comparable to only those portions of the beach that had similar beach features.

THIS PAGE INTENTIONALLY LEFT BLANK

TABLE OF CONTENTS

THIS PAGE INTENTIONALLY LEFT BLANK

LIST OF FIGURES

THIS PAGE INTENTIONALLY LEFT BLANK

LIST OF TABLES

THIS PAGE INTENTIONALLY LEFT BLANK

LIST OF ACRONYMS AND ABBREVIATIONS

2D	2 dimensional
3D	3 dimensional
CIRN	Coastal Imaging Research Network
CNA	Center for Naval Analysis
CONOPS	Concept of Operations
DJI	Da-Jiang Innovations
FAA	Federal Aviation Administration
FPS	frames per second
GCP	ground control point
GNSS	Global Navigation Satellite System
GPS	global positioning system
GWOT	Global War on Terrorism
MPWMD	Monterey Peninsula Water Management District
NAVD88	North American Vertical Datum 1988
NAVSPECWAR	Navy Special Warfare
NECC	Naval Expeditionary Component Command
OIF	Operational Iraqi Freedom
P3S	Phantom 3 Standard
RTK	real time kinematic
UAV	unmanned aerial vehicle
USCG	United States Coast Guard
USMC	United States Marine Corp
USSOCCOM	United Sates Special Operations Command
VGCP	virtual ground control points

THIS PAGE INTENTIONALLY LEFT BLANK

ACKNOWLEDGMENTS

THIS PAGE INTENTIONALLY LEFT BLANK

I.   MOTIVATION

In recent years, U.S. involvement in operations other than war, or irregular warfare (IW), has been the result of unconventional threats due to the rise in inter-state competition (Mattis 2018). Short of armed confrontations, states undermine international order through coercive behavior and efforts contesting all spectrums for dominance (Mattis 2018). The unclassified 2018 *National Defense Strategy* recognizes that continual escalation in rivalry between nations poses the greatest concern to U.S. national security (Mattis 2018).

In 2005, as a response to growing global instability, the Naval Expeditionary Component Command (NECC) was established to increase the Navy's role in support of Operation Iraqi Freedom (OIF) and also the Global War on Terrorism (GWOT) (Benbow et al. 2006). This was not the United States' first attempt at erecting riverine capabilities. The United States riverine operations date back as far as the American Revolution. They are complex, often include close combat, and involve combined arms (Benbow et al. 2006). However, between division of resources and balancing essential missions, riverine operations demise as quickly as they are established (Benbow et al. 2006). The last dedicated river operations were in Vietnam and most recently, Iraq (Benbow et al. 2006).

Inside U.S. boarders, the United States Coast Guard (USCG) has the capability to conduct security operations (Benbow et al. 2006), but outside of the country, the Navy does not maintain riverine operation as a devoted task. Prior to NECC, the navy's only riverine capable units were within Navy Special Warfare (NAVSPECWAR) (Benbow et al. 2006). As a collective military, only the United States Marine Corp (USMC) and United States Special Operations Command (USSOCOM) upheld some riverine concept of operations (CONOPS) derived from historical lessons learned (Benbow et al. 2006).

Introducing military forces in sovereign states can lead to one of three responses by the host nation and neighboring countries, permissive, uncertainty and hostile (Mattis 2018). The nature of the riverine environment extends far inland such that the U.S. can be denied access and there is no guarantee entry (Mattis 2018). With the complexity of inter-

state struggles on the rise, access denial to any part of the globe significantly reduces the U.S.' conflict management ability.

The 2006 Center for Naval Analysis (CNA) review of riverine capabilities and operations identified that there are 60 countries that fall into the non-integrated gap, Figure 1, which are regions that have the potential for U.S. involvement (Benbow et al. 2006). Together, the 60 countries accumulate over 201,000 km of waterways and 21 large river deltas, many of which are greater in scale than the Mekong Delta during the Vietnam War (Benbow et al. 2006).
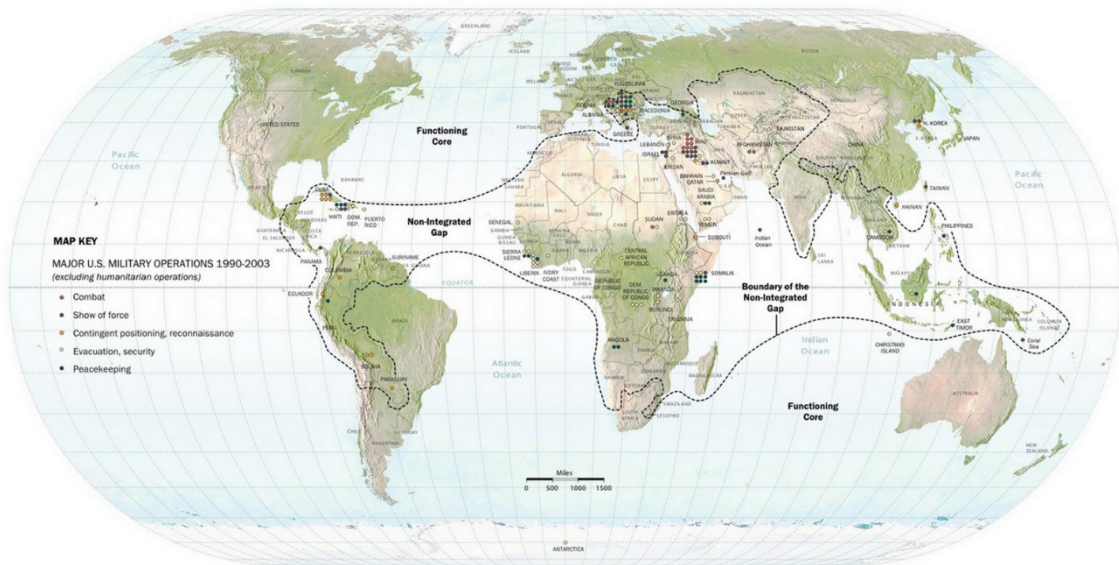
Figure 1.   CNA identified the area within the dotted line as the non-integrated gap which has the potential for U.S. involvement.
Source: Benbow et al. (2006).

IW has inetiably required the Navy to expand its exploration of maritime superiority into rivers. River waterway is an inside-out approach to gaining maritime advanage as it gives our military greater entree depth to zones where potential adversaries reside, in addition, it provides the necessary security we need to sustain peace, de-escalate conflict, and when necessary, win wars.

Traditionally, Navy Meteorology and Oceanography has supported naval operations in open ocean and along the coast. Internal waters and rivers are not the primary aquatic bodies the Navy Meteorology and Oceanography community monitors or was designed to forecast. For this reason, how will Navy Meteorology and Oceanography support brown water operations in the future?

THIS PAGE INTENTIONALLY LEFT BLANK

II.   INTRODUCTION

A.   BACKGROUND

For any marine operations, civilian or military, the most vulnerable area is the surf zone extending into the swash zone owing to the rapid changes in both morphology and wave dynamics. To date, the energetic nearshore environment continues to limit *in situ* observations. The region where waves break presents many challenges for data collection as it is unsafe for both people and equipment (Holman and Haller 2013). Numerous studies of large river discharge have been conducted, but little is understood about how small river plumes coalesce with the sea and affect the swash zone (Gatson et al. 2006). Most of the studies on swash dynamics are limited to just gently sloping or steep sandy beaches (Raubenheimer 2002; Hughes and Baldock 2004; Dodet et al. 2018), which highlights the need for understanding swash on steep and rocky beaches as well as dynamic areas of river plumes. Of particular interest for ephemeral rivers is how the river mouth ultimately closes, a process that is expected to be influenced by swash dynamics.

Carmel River State Beach presents the opportunity to observe swash behavior along a rocky shore, at a steep beach slope, and at a small river edge, all in the same setting. However, Carmel River is only open to the sea during the rainy winter months in California when lagoon water rises high enough to breach the beach berm (James 2005; Orescanin and Scooler 2018). Carmel River breaching was found to be uncorrelated to tides and wave height, but was correlated to river discharge (Orescanin and Scooler 2018). An increase in discharge while ocean forcing remains constant, or vice versa, resulted in Carmel River breaching the coastline; but at the peak of rising tides and wave heights, Carmel River also closed (Orescanin and Scooler 2018).

In this study, an unmanned aerial vehicle (UAV) quadcopter was used to observe and collect wave runup values. The measured data are compared to calculated values using empirical coefficients for smooth and rocky structure slopes developed by Ahrens (1981). The hypothesis is that wave runup is affected by the hydrodynamics of the river plume and coastal roughness. Bottom friction from rocky coastlines create the greatest resistance to

water flow compared to the pressure gradient of opposing river discharge and a steep sandy beach slope. The highest vertical runup occurs over a sandy beach and reduces over river discharge. The lowest height is expected to be over rocky shores.

The remaining portion of this chapter discusses the unique coastal features of the survey site and the use of unmanned aerial vehicles to collect data. Chapter III describes the set up and tools used to evaluate the data. Observations, findings and analysis are in Chapter IV, the results, and finally, Chapter V discusses the limitations of optical imaging along with the conclusion.

B.   SMALL AND EPHEMERAL RIVERS

Ephemeral rivers are episodic coastal waterways that open and close intermittently throughout the year. During periods of persistent or significant rainfall and water runoff, the water level in an ephemeral river rises over sand berms and allows river water to mix with the ocean (Hart 2007; Kraus et al. 2002; Orescanin and Scooler 2018). During dry seasons or periods of extended drought, the water level in an ephemeral river can diminish to where flow is minimal and the river is isolated from the sea (Hart 2007; Kraus et al. 2002; Orescanin and Scooler 2018). Oftentimes, ephemeral rivers terminate into a lagoon or perched river mouth where they deposit any remaining flow (Orescanin and Scooler 2018). When sufficient offshore pressure gradient or ocean forcing causes an imbalance in momentum, a breach joins the fresh and salt water bodies (Laudier et al. 2011, Orescanin and Scooler 2018). The cycle of water exchange is distinctive to ephemeral rivers, and at the junction point between river and ocean, the interaction can be complex. Figures 2 and 3 show Carmel River opened and closed during 2018.

Figure 2. Carmel River plume during the winter. Adapted from Google Earth (2018).

Figure 3. Carmel River closed during the summer to early fall. Adapted from Google Earth (2018).

C. SMALL RIVER DELTAS

River deltas are often influenced by the river itself, waves, and tides, but the geometry and behavior of large and small river plumes are unlike each other. The junction point between river and ocean is marked by a bulge at river exits where coastal rivers join coastal currents (Avicola and Huq 2003). River plume is characterized using the Rossby

number, which is a ratio of the river's flow compared to its length multiplied by the Coriolis force (Garvine 1988). For large-scale rivers with low Rossby numbers, the plume rotates right towards shore in the northern hemisphere (Garvine 1988); but in small rivers, right-veering plumes have not been observed. As small-scale river plumes do not display curvature, they are nonrotating (Garvine 1988) and exist without the recirculating gyres of large river plumes. The only length scale-limiting factor in small river plumes is the width of the channel (Garvin 1988).

For small rivers on wave-dominated coastlines, when the lagoon water levels increase enough, the offshore pressure gradient creates a breach through the sand berm (Warrick et al. 2007). However, the offshore pressure gradient does not necessarily continue to be the main driving factor in river flow at the river-ocean interface or beyond (Warrick et al. 2007). In a study of several small rivers in southern California, Warrick et al. (2007) found that river discharge will influence the initial offshore dynamics of the river plume, but further towards sea, transport is wind dominated. The small river plumes in southern California were observed to behave differently than that of larger river discharges and deltas (Warrick et al. 2007). Upon separation from the shore, local winds were the primary reason that river flow would speed, stall, and even reverse (Warrick et al. 2007). While many studies focus on the offshore state of river plumes, there are no studies that examine the fate of small plumes in the surf zone, and how these plumes interact and modify the swash zone.

D.   SWASH ON ROCKY SHORES

The swash zone is an area of periodic submersion and exposure by wave runup and backwash (Pitman 2014). Swash is generated by infra-gravity waves and incident waves that propagate up the beach face as a result of wave energy conversion between kinetic and potential (Erikson et al. 2007). As gravity restores the wave down the beach slope (Pitman 2014), interference between backwash and the rush of successive waves means waves often do not complete a full cycle (Erikson et al. 2007).

The parameters controlling runup are offshore wave height (H_s), wave length (L_∞) and beach slope (S) (Hunt 1959, Ahrens 1981, Komar 1998, Stockdon et al. 2006, Erikson

et al. 2007, Van de Meer and Stam 1992). Beach slope and incident waves are described using the Irribarren number (ξ), a dimensionless parameter proven effective at determining runup based on wave conditions (Dodet et al., 2018, Komar 1998, Laudier et al. 2011, Pitman 2014, Van de Meer and Stam 1992).

The Iribarren number in equation 1 was first introduced by Hunt (1959) then later rearranged to equation 2 by Battjes (1971) to describe runup.

$$\xi = \frac{S}{\sqrt{H_s / L_\infty}} \tag{1}$$

$$\frac{R_{2\%}}{H_s} = C\xi \tag{2}$$

$R_{2\%}$ is the vertical level exceeded by 2% of the runup heights and C is a dimensionless empirical coefficient. Swash heights have effective runups that create large morphological changes and significantly alter beach profiles (Pitman 2014). Runup is important to erosion and flooding indications and coastal engineering designs (Fiedler 2017). Over the years, Battjes' original equation has been improved upon by researchers and engineers to measure runup on natural beaches and coastal structures.

While wave runup has been the subject of many nearshore studies, the works of previous research have been on sandy beaches (Van de Meer and Stam 1992, Stockdon et. al 2006, Laudier et al. 2011) with little focus on rocky shores. In a study by Dodet et al. (2018), the applicability of runup formulas derived from empirical measurements were tested over steep rocky cliffs. Dodet et al. (2018) found that runup on rocky cliffs depends on the square root of the offshore significant wave heights multiply by the wave lengths. Wave runup over rocky cliffs was also depth dependent and reduced as a result of enhanced bottom friction applied to the flow (Dodet et al. 2018). Bottom roughness reduces the wave heights before the waves break, thus decreasing the wave setup as compared to smooth beach bottoms (Dodet et al. 2018). A common assumption in nearshore wave equations is that pressure is hydrostatic; Dodet et al. (2018) has accounted for unequal water column pressure distribution over rugged environment. In addition, other influences to wave runup

are changes in wave spectra, foreshore slope, and variations in the alongshore due to intertidal and subtidal bars (Dodet et al. 2018).

For the current survey site, Laudier et al.'s (2011) study of wave overtopping on Carmel River State Beach found that Stockdon et al.'s (2006) empirical values for a natural beach considerably under predicted runup for Carmel Beach. The mean grain size on Carmel Beach is .62mm (Storlazzi and Field 2000). The beach slope is steep and characterized as reflective, permeable, not barred, and influenced by incident waves (Laudier et al. 2011). The max wave angle of incident on Carmel Beach is fifteen degrees (Laudier et al. 2011) and should not induce large reduction factors for wave runup (Laudier et al. 2011). In addition, in soaked sand, resistance from surface roughness is reduced so the surface of a wet sandy beach is smooth (Laudier et al. 2011). To represent runup on Carmel River State Beach, Laudier et al. (2011) recommended using laboratory derived empirical values on similar surfaces with similar slopes. Adhering to Laudier et al.'s (2011) suggestion, Ahrens (1981) coefficients for a smooth and a rocky (rock rubble) structure were selected to compare the present measured values to.

E.   UAV FOR COASTAL SURVEYING

Conventionally, mapping and tracking river discharge and coastal environments have been accomplished using *in situ* instruments. Today, satellite remote sensing is another means to passively gather data, but at a high price. However, technology has advanced the capability to study coastal settings via a multitude of remote sensing tools and techniques. At a much lower cost, modern remote sensors share the advantage of reducing significant threat to man and equipment in the field. Remote sensing exceedingly outperforms in information exchange with large data networks and outside sources in addition to having the ability to cover an enormous amount of space at long periods (Holman and Haller 2013).

In recent years, the development and modernization of unmanned aerial vehicles have improved the ability to study coastlines with higher resolution. These remote sensors offer inexpensive environmental observations with better spatial and temporal resolution than traditional *in situ* measurements. UAVs are also effective at identifying coastal plumes

and water boundaries because of the contrast in water properties and turbidity between river water and ocean water (Klemas 2013).

Unmanned aerial vehicles with real time kinematic (RTK) global positioning system (GPS) provide high accuracy positioning with only one operator to deploy, saving survey and post processing time (Turner et al. 2016), in addition to having the capability to access coastal regions hidden from satellites. UAVs combine autonomy and computer vision to produce aerial photogrammetry of the coast (Turner et al., 2016). The components of UAVs include an autopilot navigation system, a motor for propulsion, and a battery for the digital camera (Turner et al. 2016). While UAVs have been widely used for a variety of disciplines in engineering, management, and research such as mining, firefighting, forestry, etc., it has only been recently introduced for coastal surveying (Turner et al. 2016). Holman et al. (2017) tested the accuracy and feasibility of UAVs for coast survey and found that auto piloted station keeping was within .20 and .53 m, azimuth standard deviation was within .38 degrees, and GPS position accuracy was within 5m.

THIS PAGE INTENTIONALLY LEFT BLANK

III. METHODS

A. INSPIRE 1 VERSION 2

The Da-Jiang Innovations (DJI) Inspire 1 Version 2 (Inspire) is a light airframe quadcopter with a built-in autopilot and navigations systems that are controlled via a smart phone, tablet, or laptop. The Inspire 1's camera, remote control, and battery are all interfaced to mobile devices through the DJI GO App (DJI 2017). The aerial quadcopter requires no experience for operators to fly (Turner et al., 2016) and the flight controller allows the aircraft to automatically return to the originating location in the event of a lost signal or as directed by the user (DJI 2017). Operators can plan and make flight adjustments directly into the tablet/laptop that communicates to the UAV through radio wave transmission.

Figure 4.   Inspire 1 with remote controller and batteries

The Inspire 1's feature highlights are a 4K resolution video recording camera capable of capturing 12 mega pixel still photos and is mounted on a gimbal that can be outfitted with different cameras. The Intelligent Flight Battery is an advance power management system that provides 18 minutes of flight time (DJI 2017). The DJI GO App provides live high definition video streaming from the camera over wireless communication onto a mobile device (DJI 2017). Altitude and radius limits can be set on the application to create a cylindrical geo-fence flight boundary (DJI 2017). The UAV can be manually controlled or programed to land, launch, and conduct flight plans prior to take off or while in flight (Turner et al. 2016). Even though no experience is necessary to fly the UAV, flight zones, restrictions, and regulations still apply. In the United States, the Federal Aviation Administration (FAA) requires educational users to have a remote pilot certificate and drone registration.

B.   PHOTOGRAMMETRY

In order to quantify swash runup at Carmel Beach, aerial imagery collected from the Inspire was georectified using the methods outlined by Holman et al. (2017) using single camera photogrammetry. The georectification process allows for the transformation of the real world 3-dimensional 3-D space (X,Y,Z) into 2-dimensinal (2-D) Cartesian coordinate (U,V) using camera specific properties and position and orientation in a referenced coordinate system, which can then be used to solve for the projected image geometries (Holland et al., 1997). This estimation of the geometry of objects in photography is known as photogrammetry (Holland et al. 1997). As information about the camera is necessary, prior to launching the Inspire, a camera calibration with the intended flight settings was conducted using a checkerboard with measured checker square size and the Matlab Camera Calibration Application. Camera calibration is a measurement of all the intrinsic parameters of the camera's lens, the principle point (image center), focal length, and distortion parameters. Camera calibration identifies five of the eleven unknowns to georectify an image (Holman et al. 2017).

Extrinsic parameters are the parameters that describe the position and orientation of the camera relative to the geo referenced coordinate system (Holland et al. 1997). These

14

parameters are the X_c, Y_c, and Z_c of the camera's location, the drone's GPS position and flight altitude, and the angles which describe rotation, that is the azimuth, tilt, and roll (Holman et al. 2017). These parameters make up the remaining six unknowns for georectification (Holland et al. 1997).
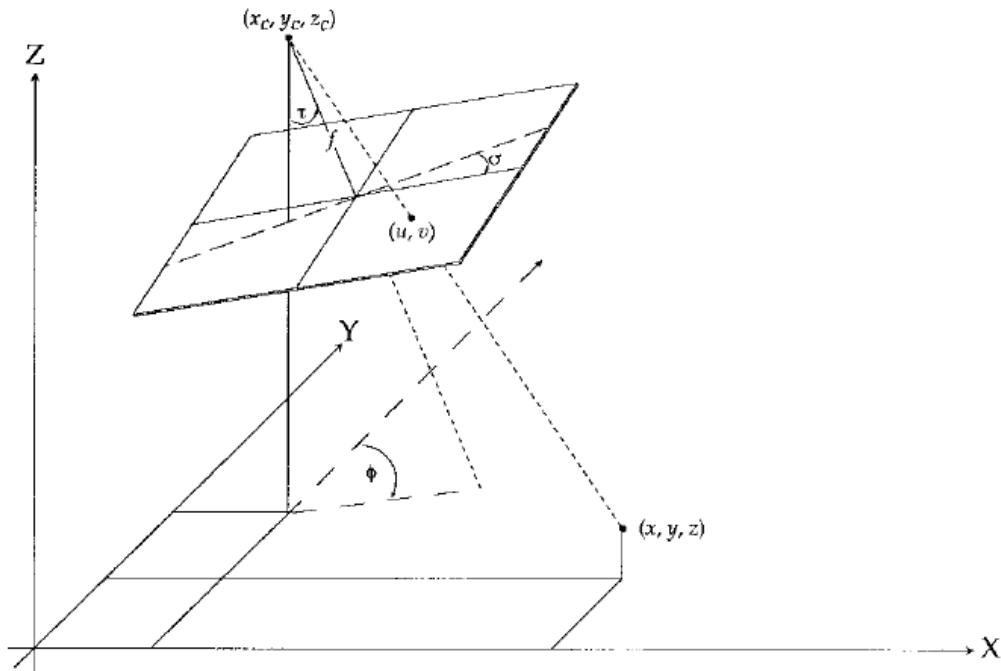
Figure 5.   Coordinate transformation between image and world coordinate.
Source: Holland et al. (1997).

Ground control points (GCP) are known locations of objects that are in the image field of view (Patria 2018) and are used to estimate extrinsic camera parameters. One GCP can determine two unknown extrinsic parameters because of the associated U and V parameters with the GCP (Holman et al. 2017). For this reason, an image can still be georectified even if the extrinsic parameters are unknown so long as there is a minimum of three GCPs to supplement (Holman et al. 2017). Holman et al. (2017), also demonstrated that increasing the number of GCPs to any number of known or unknown extrinsic parameter combinations improved transformation positional accuracy.

C.   FIELD METHODS

Wave runup was estimated using photogrammetry, an optical measurement technique in which photographs are used to approximate the geometries of the real world. Aerial observations of Carmel River State Beach took place on 23 April 2019 in Carmel, California. Wave data was extracted from the National Buoy Data Center's Point Big Sur Buoy, located approximately fourteen nautical miles offshore southwest of Carmel Beach. Carmel River flow data were taken from the Monterey Peninsula Water Management District (MPWMD) streamflow gauge station at Carmel River Highway 1 Bridge.

Ground control points consisted of 1m by 1m wooden boards painted with a black four-square checker board pattern. Figure 7 is an image of a GCP during the survey. Ground control points were placed on both sides of the river. GCP locations were in proximity of the river mouth and had to be in the Inspire's field of view during flight. No GCPs were affixed at Carmel River State Beach because of the high wave and wind conditions. GCPs were deployed and GCP positions were surveyed with two Spectra SP60 Global Navigation Satellite System (GNSS) receivers, both with horizontal accuracy within 3mm and vertical accuracy within 3.5mm. The SP60 receivers were placed in the center of each GCP for five to ten minutes, collecting GPS data, and later averaged for a single fix position. The same GPS receivers were also mounted to a pole that was strapped to a backpack, and carried for the beach walking survey seen in Figure 8. Walking survey lines were shore normal and spaced between 1 to 3 meters apart. All vertical data were referenced or converted to the North American Vertical Datum 1988 (NAVD88). Linear regression lines over the elevation data collected were used to determine beach slopes.
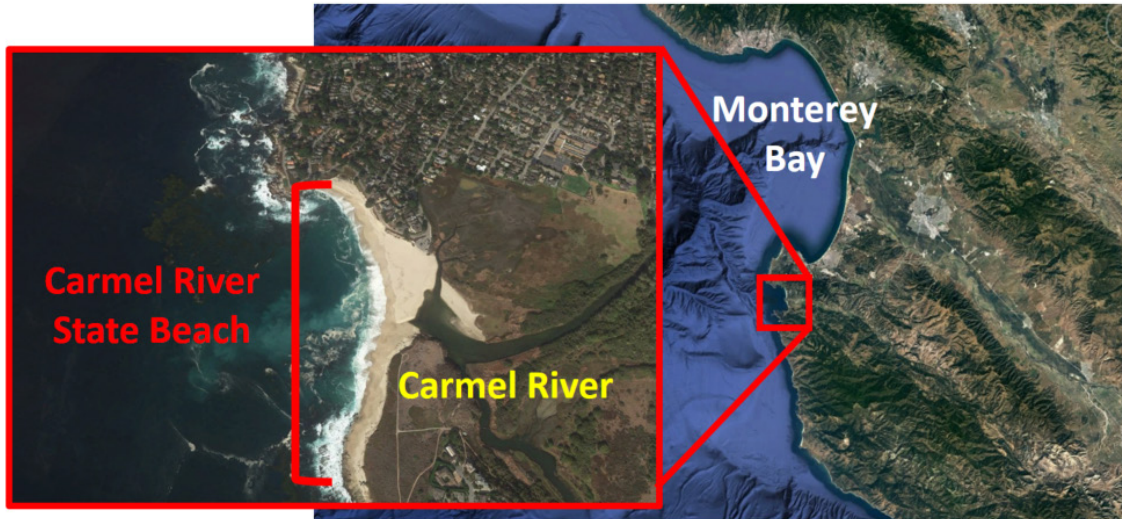
Figure 6.   Carmel River State Beach when the Carmel River is closed off
from the sea. Adapted from Google Earth (2018).

Figure 7.   A ground control point along the Carmel River

Figure 8.   Walking survey on Carmel River State Beach

D.   DATA PROCESSING

The Inspire was launched over the survey site and set to hover for five to fifteen minutes in duration. Post recovery, the Inspire's recorded videos were downloaded and decimated to 2 Hz still frames to track waves and swells (Patria 2018). Our Inspire data processing approach followed that of Patria's (2018), using the methods by Holman et al. (2017). Our analysis techniques were derived from the methods in the Coastal Imaging Research Network's (CIRN) UAV Processing Toolbox (CIRN 2019).

The UAV Processing Toolbox automates small shift recognition in drone position while hovering. These small shifts are detected using color intensity contrast of features users identify in the first photo frame, known as virtual GCPs (VGCP) (Holman et al. 2017). VGCPs are not the same as GCPs (Patria 2018), which are known surveyed positions of points in a photograph. VGCPs are features present in the field of view in all the frames that users manually identify. VGCPs in the first frame are used to calculate a reference geometry that is applied to the remaining frames in a video, which then accounts for any inflight positional changes in the quadcopter (Holman et al. 2017). In this survey, our GCPs were reused as VGCPs due to their unique board pattern which easily isolates

18

the features from the background. Once GCPs and VGCPs were identified, georectified images were produced.

The georetified images were averaged over the flight duration to produce the time exposure image in Figure 9 (Holland et al. 1997).
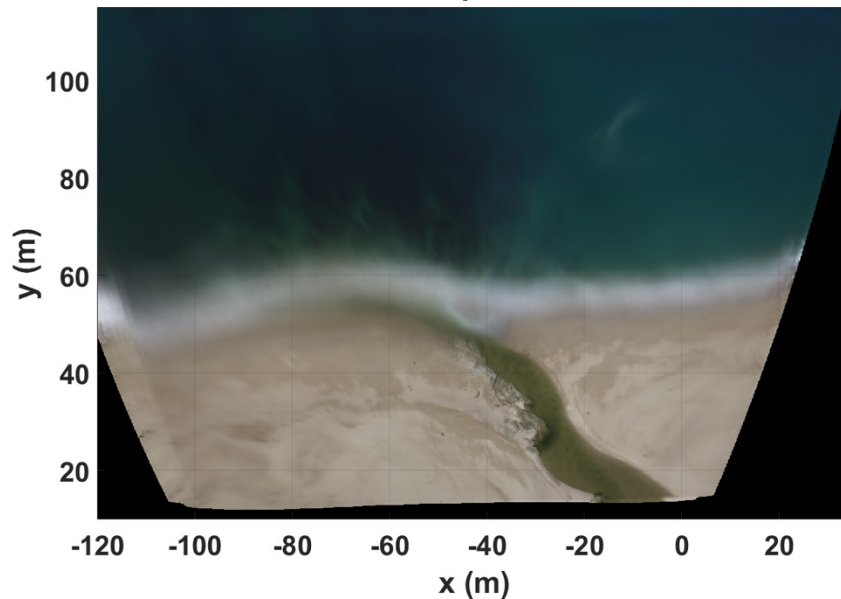
Figure 9. Swash time average of Carmel River State Park in local coordinate system

In Figure 10, transects over the sandy portion of the beach, the river mouth, and the rocky shoreline were identified for time stack image analysis. In Figure 11, the runup onshore in each transect was extracted using pixel intensity to create a runup front. From this runup front, we use Matlab algorithms to find the furthest onshore distances. To find the R2%, the highest onshore peaks were divided by the total runup. R2% values were then correlated with the beach elevation from the walking survey in Figure 12 to determine the vertical R2% heights.

Figure 10.   Survey transect lines
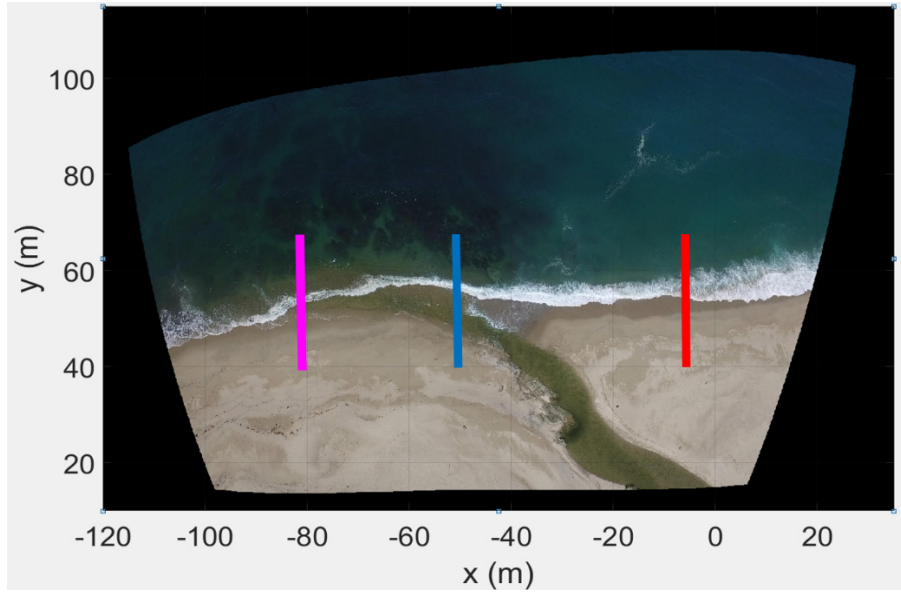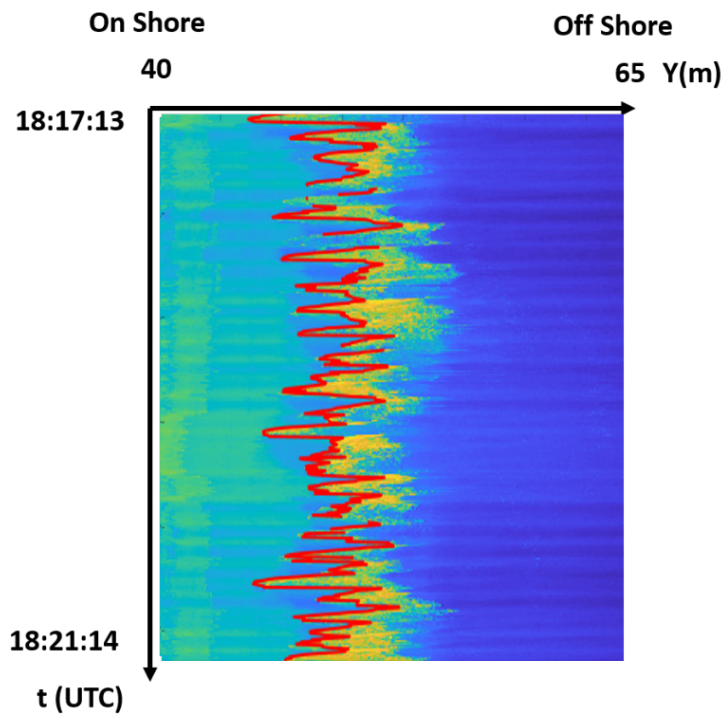

Figure 11.   Cross shore line over sandy portion of Carmel River State Beach
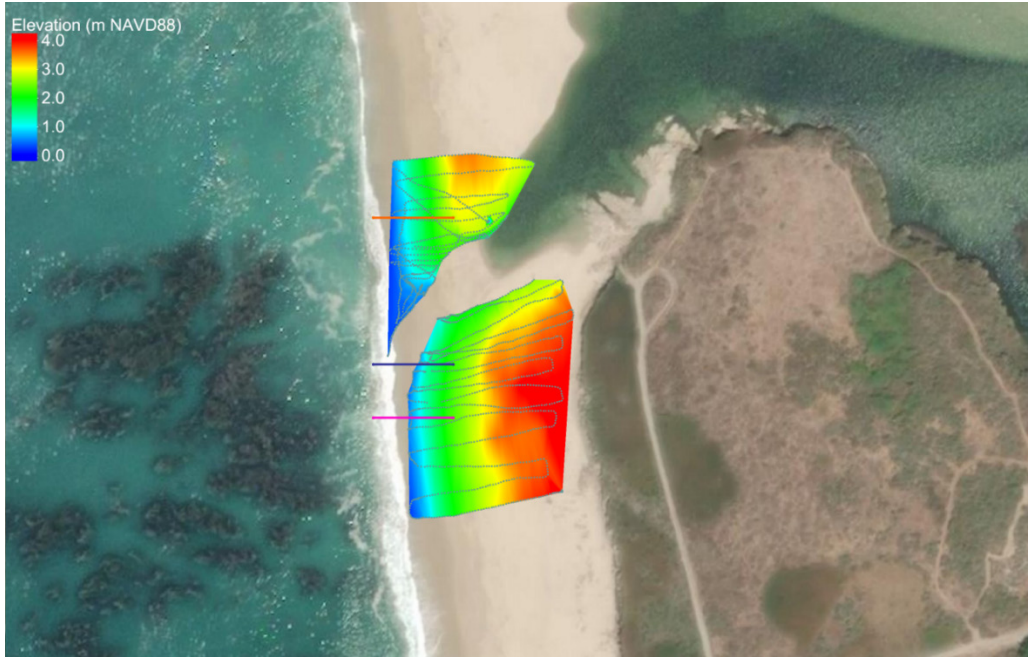
Figure 12.   Transect and beach elevation correlation

THIS PAGE INTENTIONALLY LEFT BLANK

IV. RESULTS

The elevation of Carmel River State beach is highest in the north and lowers by half a meter to one meter near the river and towards the south. Elevation data from the walking survey shown in Figure 13 were consistent and in good agreement with first order linear regression goodness of fit lines. Data from the north cross shore line and the south cross shore line aligned closely with their perspective fit lines. Data from the center cross shore line showed the greatest variation in beach elevation.
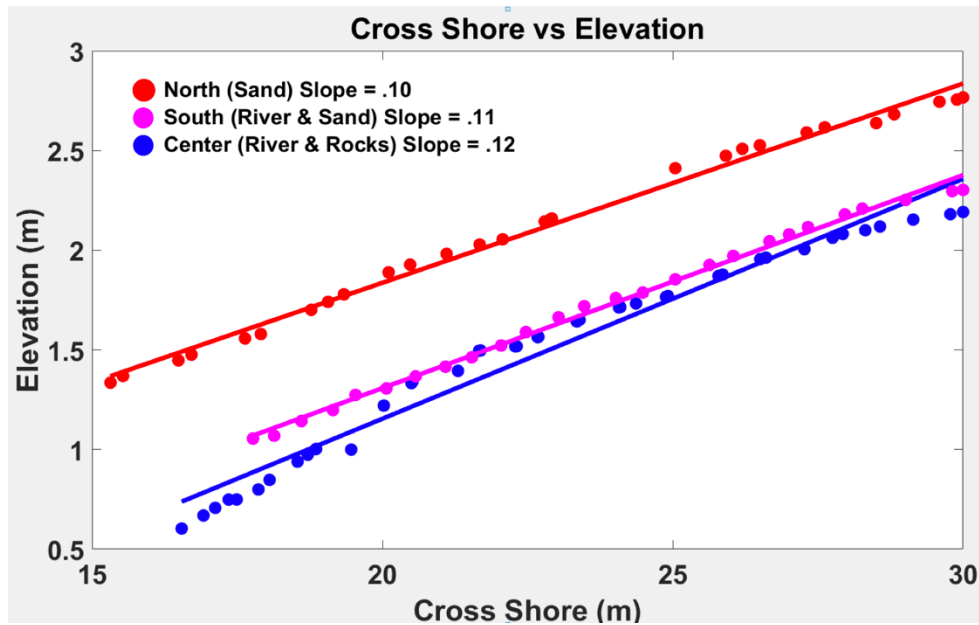
Figure 13. Cross shore elevation data with linear regression lines and slopes

The overall average slope of Carmel River State Beach is .11. The beach is steep and the slopes are consistent along shore with very small deviation from the mean. The highest beach slope occurs closest to the river while the shallowest slope is the northern portion of the beach.

Table 1 is the metadata from 23 April 2019. Wave heights off shore at the Big Sur Buoy were less than two meters. During the time of survey, the tidal phase was a flood at

a level of .6 meter. Carmel River discharge flow gauge at Highway 1 Bridge recorded low river flow at 3.48 cubic meters per second.

Table 1.   Metadata. Adapted from NBDC (2019), NOAA (2018), and MPWMD (2019).

Data	Measured Value
Significant Wave Height (Big Sur Buoy)	1.8 m
Tide (NAVD88) (Monterey Tide Gauge)	.6 m
Carmel River Discharge (Highway 1 Bridge)	3.48 m³/s

Table 2 shows the measured runup values along with calculated values for a smooth and rocky structure slope using Ahrens' (1981) empirical coefficients. The measured runup values were low compared to smooth surface but higher than that of a rocky surface. As theoretically and empirically runup heights increase with steepening beach slope, the measured runup values did not follow the same trend. The lowest runup height was at the steepest portion of the beach where sand and river discharge were.

Table 2.   Calculated vertical R2% using empirical coefficients and measured vertical R2%

Transect	Beach Slope	ξ	R2% Smooth (C=1.61) (m)	R2% Measured (m)	R2% Rocky (Rock Rubble) (C=.84) (m)
North (Sand)	.10	1.04	3.02	2.92	1.58
South (River & Sand)	.11	1.11	3.22	2.63	1.68
Center (River & Rocks)	.12	1.25	3.63	2.33	1.90

Table 3 compares the calculated vertical R2% using Ahrens' (1981) coefficients for smooth and rocky structured slopes with that of the measured vertical R2% at Carmel

River State Beach. The sandy portion of the beach compared closely to that of a smooth structure but did not compare well with a rocky structured slope. Over river discharge and sand combined, runup heights lowered, but the greatest runup difference between surface types is amid the measured value and a rocky surface. With river and rocks, runup heights decreased even further, and the largest runup difference between surface types is between the observed value and a smooth surface.

Table 3.   Comparison between calculated vertical R2% using empirical
coefficients and measured vertical R2%

Transect	R2% Measured - Smooth (m)	R2% Measured - Rocky (m)
North (Sand)	-.10	1.34
South (River & Sand)	-.59	.95
Center (River & Rocks)	-1.30	.43

THIS PAGE INTENTIONALLY LEFT BLANK

V. DISCUSSION AND CONCLUSION

A. LIMITATIONS OF COLOR CONTRAST

Although video imaging outperforms in gathering spatial and temporal resolutions and time series data (Bailey and Shand 1994), there are still limitations. Remote sensors are susceptible to environmental conditions and are particularly limited by atmosphere changes, which affects the quality of the image (Pitman 2014). Despite that data collected in this experiment occurred over a relatively short period, survey time near sunset were avoided because of sun glare and light over exposure in videos and pictures. Sun angle is extremely important and can obscure image pixel intensity by creating shifts in camera tilt and exaggeration of real world features and motion (Pitman 2014).

While color contrast analysis was effective in locating the leading edge of well-defined runup profiles, it was not useful in regions where color difference is not as sharp, such as in finding trailing swash edges or backwashes (Pitman 2014, Almar et al. 2017). This reliability on color disparity prevents swash analysis from being automated and requires manual analysis as a temporary solution, which is not only a subjective process (Bailey and Shand 1994), but is also inefficient with large data sets.

Image analysis is useful for capturing flow reversal time series but does not describe the internal flow hydrodynamics of the swash zone (Power et al. 2011). In this study, both visual and infrared data recording were attempted, but due to the time of the year the survey was conducted, there was not enough temperature difference between Carmel River Lagoon water and coastal water to use color contrast analysis. However, during the summer to late fall, water temperatures in the lagoon may be warm enough to provide better infrared imaging.

B. TRAPPED COASTAL PLUME

Although infrared data gathered could not be quantitatively analyzed, the infrared videos recorded added value in identifying river plume location and show relative temperature values to 0.1 ºC accuracy. Figure 14 is an infrared image showing Carmel River interface with the ocean. The image shows that the northern portion of Carmel River State Beach is free of

river water and that the river's discharge is constrained and bounded by the surf zone and the beach, trapping the river plume along the coast.
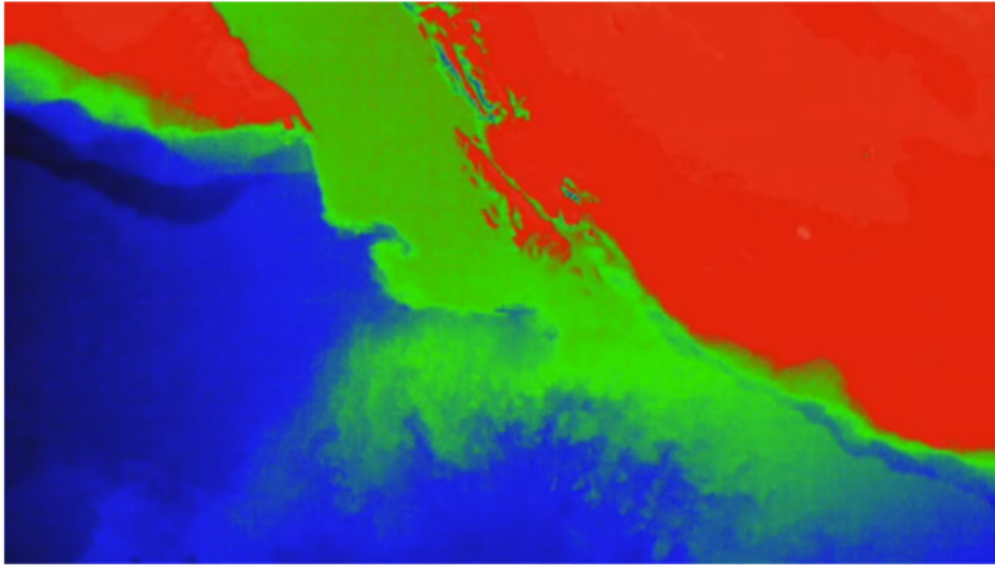

Figure 14.   Infrared Image of Carmel River Plume trapped along the coast. In red is the sand, green is the Carmel River, and blue is the Pacific Ocean.

This observed phenomenon recounts another peculiar characteristic about small river plume behavior which distinguishes them from large river deltas. Although we did not gather wind data to correlate river discharge with, our qualitative infrared records of Carmel River showed variable plumes independent of Coriolis circulations, which agrees with Warrick et al. (2007)'s account of southern California river plumes. While Carmel River was low flowing during our survey, river plume path is critical because it has implications for beach erosion, breach closure mechanisms, and sediment transport. How would higher river flow rate affect vertical runup height, and would the river plume still be trapped along the coast?

C.   SIGNIFICANCE OF VARIABLE RUNUP ALONG THE BEACH

Ease of wave runup over certain areas of the beach raises questions about breaching, sediment transport, and erosion. The area of particular interest is the northern sandy portion of beach. Laudier et al.'s (2011) study of wave overtopping at Carmel River State Beach

focused on the broad topic at large and did not specify where on the beach they expect overtopping to occur. Our data suggests that if wave runup is highest to the northern portion of Carmel Beach, it should be the mostly likely place for sea water intrusion to occur. However, it is also possible that if the river breaches to the north on Carmel Beach, depending on the strength of river flow, the river may induce enough reduction factor to wave runup such that it reduces wave overtopping. Without measured data to compare, there can be many speculations and further investigation is required to accept or reject these assumptions.

D.   NAVAL APPLICATION

There is a spectrum of operations in the U.S. Navy that can benefit from UAV swash and runup analysis on the coast. The independent remote sensors allow runup heights to be calculated anywhere in the world where weather conditions permit. This is beneficial to Naval Special Warfare, Amphibious Warfare, and the United States Marine Corp in decision making and when determining the best locations to beach vehicles, personnel, and equipment. Knowing the characteristics of runup over river deltas provide Coastal Riverine Squadrons the opportunity to establish safety measures and boat handling techniques for security patrols. In the same way, infrared video recordings of river plume can guide mine sweepers and Explosive Ordinance Disposal units to mines if they can anticipate particle trajectories based on river plume. Finally, swash and runup height are important to Naval Civil Engineering when constructing piers and fleet support facilities.

E.   CONCLUSION

Runup is affected by the hydrodynamics of river plume and coastal topography by lowering the vertical runup level. Contrary to Battjes' relationship between wave height and beach slope, near Carmel River plume, the greatest slope does not yield the highest vertical runup height. The highest runup was observed on the sandy portion of beach, trailed by over river discharge and sand, then river discharge and rocks. The empirical values developed by Ahrens (1987) over smooth and rocky slopes compared better in those portions of the beach which had similar beach features. It is inconclusive between river and rocks which had greater effect on runup height, but increasing the roughness of the beach face reduces vertical runup height regardless of increasing slope.

THIS PAGE INTENTIONALLY LEFT BLANK

LIST OF REFERENCES

Ahrens, J.P., 1981: Irregular wave runup on smooth slopes. Technical Aid No. 81–17, Coastal Engineering Research Center, Waterways Experiment Station, Vicksburg, MS.

Almar, R., C. Blenkinsopp, L. P. Almeida, R. Cienfuegos, and P. A. Catalán, 2017: Wave runup video motion detection using the Radon Transform. Coastal Engineering, 130, 46–51, https://doi.org/10.1016/j.coastaleng.2017.09.015.

Avicola, G., and P. Huq, 2003: The characteristics of the recirculating bulge region in coastal buoyant outflows. Journal of Marine Research, 61, 435–463, https://doi.org/10.1357/002224003322384889.

Bailey, D. G., and R. D. Shand, 1994: Determining Wave Run-Up Using Automated Video Analysis. Proceedings of the Second New Zealand Conference on Image and Vision Computing, 2, 1–2.

Battjes, J.A., 1971: Run-up distributions of waves breaking on slopes. Journal of Waterways and Harbors Division, 97, 1, 91–114.

Benbow, R., R., F. Ensminger, P. Swartz, S. Savitz, and D. Stimpson, 2006: Renewal of Navys Riverine capability: A preliminary examination of past, current and future capabilities. CRM D001 3241. A5/2Rev, 188, https://doi.org/10.21236/ada447820.

CIRN, 2019: CIRN: Coastal Imaging Research Network. Accessed 18 April 2019, https://coastal-imaging-research-network.github.io/#.

Dodet, G., F. Leckler, D. Sous, F. Ardhuin, J. Filipot, and S. Suanez, 2018: Wave Runup Over Steep Rocky Cliffs. Journal of Geophysical Research: Oceans, 123, 7185–7205, https://doi.org/10.1029/2018JC013967.

Erikson, L., M. Larson, and H. Hanson, 2005: Prediction of swash motion and run-up including the effects of swash interaction. Coastal Engineering, 52, 285–302, https://doi.org/10.1016/j.coastaleng.2004.12.001.

Fiedler, J. W., P. B. Smit, K. L. Brodie, J. Mcninch, and R. Guza, 2018: Numerical modeling of wave runup on steep and mildly sloping natural beaches. Coastal Engineering, 131, 106–113, https://doi.org/10.1016/j.coastaleng.2017.09.004.

Garvine, G.W., 1988: Estuary plumes and fronts in shelf waters: a layer model. Deep Sea Research Part B. Oceanographic Literature Review, 35, 524, https://doi.org/10.1016/0198-0254(88)92398-9.

DJI, 2017: Phantom 3 Standard. User Manual, 54, https://dl.djicdn.com/downloads/phantom_3/User%20Manual/Phantom_3_Standard_User_Manual_v1.4_en.pdf.

Google Earth, 2018. Accessed 18 April 2019, https://earth.google.com/web.

Hart, D. E., 2007: River-mouth lagoon dynamics on mixed sand and barrier coasts. J. Coastal Res, 927–931.

Holland, K., R. Holman, T. Lippmann, J. Stanley, and N. Plant, 1997: Practical use of video imagery in nearshore oceanographic field studies. IEEE Journal of Oceanic Engineering, 22, 81–92, https://doi.org/10.1109/48.557542.

Holman, R. A., K. L. Brodie, and N.J. Spore, Jr., 2017: Surf Zone Characterization Using a Small Quadcopter: Technical Issues and Procedures. IEEE Journals & Magazine, 55, 4, 2017–2027.

Holman, R., and M. C. Haller, 2013: Remote Sensing of the Nearshore. Annual Review of Marine Science, 5, 95–113, https://doi.org/10.1146/annurev-marine-121211-172408.

Hughes, M. G., & Baldock, T. E., 2004: Eulerian flow velocities in the swash zone: Field data and model predictions. Journal of Geophysical Research: Oceans, 109, C8, https://doi.org/10.1029/2003jc002213.

Hunt, I. A., 1959: Design of Sea-Walls and Breakwaters. Transactions of the American Society of Civil Engineers, 126, 4, 542–570.

James, G. W., 2005: Technical Memorandum 05–01: Surface Water Dynamics at the Carmel River Lagoon Water Years 1991 Through 2005, 44.

Klemas, V., 2013: Airborne Remote Sensing of Coastal Features and Processes: An Overview. Journal of Coastal Research, 287, 239–255, https://doi.org/10.2112/jcoastres-d-12-00107.1.

Komar, P.D., 1998: Beach Processes and Sedimentation. Prentice Hall, 544.

Kraus, N.C., A. Militello, and G. Todoroff, 2002: Barrier breaching processes and barrier spit breach, Stone Lagoon, California, Shore & Breach, 70, 4, 21–28.

Laudier, N. A., E. B. Thornton, and J. MacMahan, 2011: Measured and molded wave overtopping on a natural beach. Coastal Engineering, 58, 9, 815–825, https://doi.org/10.1016/j.coastaleng.2011.04.005.

Mattis, J.N., 2018: National Defense Strategy 2018. National Security Strategy Archive, Accessed 18 April 2019, http://nssarchive.us/national-defense-strategy-2018.

MPWMD, 2019: Carmel River Flows. Accessed 13 May 2019, https://www.mpwmd.net/environmental-stewardship/carmel-river-basin/carmel-river-flows.

NDBC, 2019: Station 46239 – Point Sur, CA (157). National Oceanic and Atmospheric Administration, Accessed 13 May 2019, https://www.ndbc.noaa.gov/ station_page.php?station=46239.

NOAA, 2018: Tides and Currents. Accessed 14 May 2019, https://tidesandcurrents.noaa.gov/noaatidepredictions.html?id=9413450&legacy=1.

Orescanin, M. M., and J. Scooler, 2018: Observations of episodic breaching and closure at an ephemeral river. Continental Shelf Research, 166, 77–82, https://doi.org/10.1016/ j.csr.2018.07.003.

Patria, N. S., 2018: Optical Kinematics of Wave-Swept Surge Channel Rip Currents. Naval Postgraduate School Monterey United States, 53, https://apps.dtic.mil/dtic/tr/fulltext/ u2/1069686.pdf.

Pitman, S.J., 2014: Methods for field measurement and remote sensing of the swash zone. Geomorphological Techniques, British Society for Geomorphology, 3–2.

Power, H. E., R. A. Holman, and T. E. Baldock, 2011: Swash zone boundary conditions derived from optical remote sensing of swash zone flow patterns. Journal of Geophysical Research: Oceans, 116, C6, https://doi.org/10.1029/2010JC006724.

Raubenheimer, B., 2002: Observations and predictions of fluid velocities in the surf and swash zones. Journal of Geophysical Research, 107, C11, 11–1, https://doi.org/ 10.1029/2001jc001264.

Stockdon, H.F., Holman, R.A., Howd, A.H., Sallenger, A.H., 2006: Empirical parameterization of setup, swash, and runup. Coastal Engineering, 53, 7, 573–588, https://doi.org/10.1016/j.coastaleng.2005.12.005.

Storlazzi, C.D., Field, M.E., 2000. Sediment distribution and transport along a rocky, embayed coast: Monterey Peninsula and Carmel Bay, California. Marine Geology, 170, 3–4, 289–316, https://doi.org/10.1016/S0025-3227(00)00100-6.

Turner, I. L., C. Drummond, M.D. Harley, 2016: UAVs for coastal surveying. Coastal Engineering, 114, 19–24, https://doi.org/10.1016/j.coastaleng.2016.03.011.

Van der Meer, J. W., and Stam, C. J. M., 1992: Wave runup on smooth and rock slopes of coastal structures. Journal of Waterway, Port, Coastal, and Ocean Engineering, 118, 5, 534–550, https://doi.org/10.1061/(ASCE)0733-950X(1992)118:5(534).

Warrick, J., and Coauthors, 2007: River plume patterns and dynamics within the Southern California Bight. Continental Shelf Research, 27, 19, 2427–2448, https://doi.org/ 10.1016/j.csr.2007.06.015.

THIS PAGE INTENTIONALLY LEFT BLANK

INITIAL DISTRIBUTION LIST

1.   Defense Technical Information Center
      Ft. Belvoir, Virginia

2.   Dudley Knox Library
      Naval Postgraduate School
      Monterey, California